Role of centrality for the identification of influential spreaders in complex networks

Physical Review E, College Park, v.90, n.3, p.032812-1-032812-17, 2014
http://www.producao.usp.br/handle/BDPI/46331

Role of centrality for the identification of influential spreaders in complex networks

Guilherme Ferraz de Arruda, André Luiz Barbieri, Pablo Martín Rodríguez, and Francisco A. Rodrigues*
Departamento de Matemática Aplicada e Estatística, Instituto de Ciências Matemáticas e de Computação, Universidade de São Paulo, Campus de São Carlos, Caixa Postal 668, 13560-970 São Carlos, SP, Brazil

Yamir Moreno
Institute for Biocomputation and Physics of Complex Systems (BIFI) & Department of Theoretical Physics, University of Zaragoza, 50018 Zaragoza, Spain and Complex Networks and Systems Lagrange Lab, Institute for Scientific Interchange, Turin, Italy

Luciano da Fontoura Costa
Instituto de Física de São Carlos, Universidade de São Paulo, Av. Trabalhador São Carlense 400, Caixa Postal 369, CEP 13560-970, São Carlos, São Paulo, Brazil

(Received 12 April 2014; revised manuscript received 28 July 2014; published 22 September 2014)

The identification of the most influential spreaders in networks is important to control and understand the spreading capabilities of the system as well as to ensure an efficient information diffusion such as in rumorlike dynamics. Recent works have suggested that the identification of influential spreaders is not independent of the dynamics being studied. For instance, the key disease spreaders might not necessarily be so important when it comes to analyzing social contagion or rumor propagation. Additionally, it has been shown that different metrics (degree, coreness, etc.) might identify different influential nodes even for the same dynamical processes with diverse degrees of accuracy. In this paper, we investigate how nine centrality measures correlate with the disease and rumor spreading capabilities of the nodes in different synthetic and real-world (both spatial and nonspatial) networks. We also propose a generalization of the random walk accessibility as a new centrality measure and derive analytical expressions for the latter measure for simple network configurations. Our results show that for nonspatial networks, the k-core and degree centralities are the most correlated to epidemic spreading, whereas the average neighborhood degree, the closeness centrality, and accessibility are the most related to rumor dynamics. On the contrary, for spatial networks, the accessibility measure outperforms the rest of the centrality metrics in almost all cases regardless of the kind of dynamics considered. Therefore, an important consequence of our analysis is that previous studies performed in synthetic random networks cannot be generalized to the case of spatial networks.

DOI: 10.1103/PhysRevE.90.032812 PACS number(s): 89.75.Hc, 89.75.Kd

I. INTRODUCTION

Spreading phenomena are ubiquitous in nature [1,2]. Rumors and viruses spread from person to person, worms contaminate computers worldwide, and innovations are diffused from place to place. The advent of new technology and modern transportation means has led to radical changes of classical transmission channels, making, in many cases, natural and humanmade systems more prone to contagion processes. On the other hand, new tools have been developed to study such phenomena, for instance, by explicitly dealing with the topology and dynamics of so-called complex networks, which are nothing but the backbone on top of which information and diseases propagate [3,4].

Networks are composed of nodes, which represent the elements of the system, and edges, which define the possible interaction patterns among nodes [5,6]. A large body of recent studies has verified that the way in which such nodes are organized plays a fundamental role in spreading processes [6,7]. For instance, Pastor-Satorras and Vespignani showed that a disease outbreak takes place when the spreading rate, β, is larger than the epidemic threshold [8], i.e., if $\beta > \beta_c = \langle k \rangle / \langle k^2 \rangle$, where $\langle k^m \rangle$ is the m-th moment of the degree distribution. Therefore, most scale-free networks (those for which the degree distribution follows a power law $P(k) \sim k^{-\gamma}$ with $\gamma < 3$) are particularly prone to the spreading of diseases, since $\beta_c \to 0$ when $N \to \infty$. Additional network properties, such as assortativity [9,10] or modular organization [11], also play a fundamental role in disease spreading.

One of the most interesting challenges in network science is to understand the relation between the structure of the system and its emergent dynamical properties. This is why finding determinant structural factors is important, as a better knowledge would allow controlling the function of the system, which for the scope of this paper, means determining what network properties are more closely related to information and viruses diffusion. In particular, we will focus our attention in one topological feature: centrality. Since the most central nodes can diffuse their influence to the whole network faster than the rest of nodes, it is expected that such agents are the most influential spreaders. Recently, Kitsak *et al.* [12] found evidence that confirmed this hypothesis for the case of epidemic outbreaks. The authors verified that the most influential spreaders can be forecasted from the k-shell decomposition analysis. Such agents are located within the core of the network and do not need to be the most connected. Silva *et al.* [13] explored the correlations between heterogeneous

*francisco@icmc.usp.br

spread and central attributes of the vertices that were first seeded with a disease, finding that degree and accessibility are measures mostly related to the efficient spread of the disease. On the other hand, Borge-Holthoefer and Moreno [14] showed that, for standard rumor models, it is not possible to identify the most influential spreaders using the same metrics.

Although many works have provided evidence for the presence of influential spreaders in epidemic spreading, the conclusions are not general. Indeed, there is no general consensus on the definition of network "centrality," because there are many measures able to quantify the centrality of a node, each one considering specific concepts [4]. For instance, the betweenness and closeness centrality take into account only the shortest distance between pairs of nodes [4,6], ignoring alternative paths. At the same time, the k-core decomposition may eliminate important sets of vertices, which can be connected to the main core through nodes with a small number of links [15]. Thus, to overcome such a lack of a universal definition of node centrality, it is necessary to look at additional measures. In this paper, we study the problem of the identification of influential spreaders using eight centrality measures in order to complement previous studies [12,14]. Moreover, we introduce a new metric, the generalized accessibility, as a centrality measure that is based on random walks. We observe that in social and scale-free networks, the accessibility, average neighborhood degree, and closeness centrality are the measures most related to rumor spreading. Other measures, such as the k-core and degree, correlate well only with epidemic spreading in social networks, as found previously in Refs. [12,14].

Another important result is related to the kinds of networks studied in this work. Despite the fact that many diffusion processes take place on spatially embedded networks [16], previous studies have disregarded spatial networks [12–14]. These networks have several topological constraints that greatly influence the way that connections are established, and thus, one expects an impact in network centrality metrics and, consequently, on the spreading dynamics. In this paper, we intend to fill this gap by exploring the role of centrality measures in predicting the spreading capabilities of nodes of spatial networks. Specifically, we consider both real networks (road networks of four countries) and artificial spatial networks with exponential and power-law degree distributions and find that correlations between spreading capacity and centrality measures in spatial networks differs significantly from those observed in nonspatial networks.

This paper is organized as follows. Section II presents the centrality measures considered in our investigations. The generalized random walk accessibility is introduced in Sec. III. The analytical expressions for complete graphs, stars, and rings are also evaluated in this section. Concepts of epidemic and rumor spreading are discussed in Sec. IV and the databases are described in Sec. V. The analysis of spatial networks is outlined in Sec.VII, where it is shown that the accessibility is strongly correlated to the node capacity for rumor and epidemic spreading. Section VIII presents the analysis of nonspatial networks, which complements the investigations in Refs. [12,14]. Our final conclusions are developed in Sec. IX.

II. CENTRALITY MEASURES

As mentioned before, one can in principle consider several metrics to define the centrality of a node [4]. For completeness, here we provide the basic definitions of those that will be used in the rest of the paper. For more details, we refer the reader to the literature cited.

a. Connectivity-based centrality measures. The most basic definition of centrality takes into account the number of connections of a node i, called node degree, k_i. In this case, the most central node has the largest number of connections. Alternatively, the centrality of a vertex can be defined in terms of the degree of its second neighbors, since strongly connected vertices can surround a central node. In this case, the average degree of the nearest neighbors of i is defined as

$$r_i = \frac{1}{k_i} \sum_{j \in \nu(i)} k_j, \tag{1}$$

where $\nu(i)$ is the set of nodes connected to i. It has been verified that the average neighborhood degree is related to epidemic spreading in networks [3].

b. Eigenvector centrality. It considers that the centrality of each node is the sum of the centrality values of the nodes that it is connected to. The eigenvector centrality is defined by the eigenvector associated to the largest eigenvalue of the adjacency matrix A. Formally,

$$x_i = \kappa^{-1} \sum_j A_{ij} x_j, \tag{2}$$

or, in the matrix form, $A\mathbf{x} = \kappa \mathbf{x}$, where $\mathbf{x}$ is the right leading eigenvector [4] and κ is the largest eigenvalue.

c. Distance-based centrality metrics. Centrality can also be established in terms of the shortest distances between pairs of nodes, since the more central a node is, the lower its total distance to all other nodes is. The closeness centrality of i is defined as [4]

$$C_i = \frac{N}{\sum_{j=1, j \neq i}^{N} d_{ij}}, \tag{3}$$

where d_{ij} is the shortest distance between nodes i and j, and N is the number of nodes in the network.

Alternatively, the effective load of a node can also be considered as a centrality measure. Betweenness centrality quantifies the load as the number of times a node acts as a bridge along the shortest path between two other nodes [17]. Thus, for a node i,

$$B_i = \sum_{(a,b)} \frac{\sigma(a,i,b)}{\sigma(a,b)}, \tag{4}$$

where $\sigma(a,i,b)$ is the number of shortest paths connecting vertices a and b that pass through vertex i and $\sigma(a,b)$ is the total number of shortest paths between a and b. The sum is over all pairs (a,b) of distinct vertices. In this case, a central node is crossed by many paths and shows the highest value of B_i.

d. Clustering. The clustering coefficient quantifies the occurrence of triangles in the networks. It is defined as [6]

$$\mathrm{cc}(i) = \frac{N_{\triangle}(i)}{N_3(i)}, \tag{5}$$

where $N_{\triangle}(i)$ is the number of triangles involving the node i and $N_3(i)$ is the number of triples centered around i. $\mathrm{cc}(i)$ can be also understood as a centrality measure in the sense that if two nodes are connected only via the node i, this node can control the information flow [4]. Thus, the clustering coefficient could be thought off as a local version of the betweenness centrality. Note that $\mathrm{cc}(i)$ takes smaller values for more central nodes, in opposite to the other centrality measures.

e. Coreness. The k-shell decomposition partitions a network into substructures and assigns an integer index to each node i, $k_c(i)$, in such a way that $k_c(i) = k$ if i belongs to the k-core, but it is not in the $(k+1)$-core [15]. Nodes with low values of k_c are located at the periphery of the network. This measure was adopted recently to detect influential spreaders in networks [12]. The most central nodes should have the highest values of coreness, whereas high-degree nodes localized in the periphery of networks should display small values of coreness [12]. Therefore, only hubs at the main core of networks present the highest values of k_c.

f. Random-walk based centrality measures. The number of visits that a given node receives when an agent travels through the network without a preferential route can also be taken into account to quantify the node centrality. In this case, a possible measure is the Google PageRank [18]. PageRank is calculated as

$$\pi^T = \pi^T G, \tag{6}$$

where G is the Google matrix, i.e.,

$$G = \kappa\left(P + \frac{ae^T}{N}\right) + \frac{(1-\kappa)}{N}ee^T, \tag{7}$$

and a is the binary vector called dangling node vector (a_i is equal to 1 if i is a dangling node and 0 otherwise), e is a vector of ones of length N, and P is the transition probability matrix of the respective network [$P(i,j) = \frac{1}{\sum_j A_{ij}}$, where A_{ij} are the elements of the adjacency matrix]. The original version of the algorithm considers $\kappa = 0.85$ [18]. The PageRank of a node i, π_i, is given by the i-th entry of the dominant eigenvector π of G, given that $\sum_i \pi_i = 1$. π_i can be understood as the probability of arriving at the node i after a large number of steps following a random walk navigation through the network.

III. GENERALIZED RANDOM WALK ACCESSIBILITY

The accessibility is related to the diversity of access of individual nodes through random walks [19]. This measure has been considered for identification of the border of complex networks [20]. Let $P^{(h)}(i,j)$ be the probability of reaching node j by performing random walks of length h departing from i. The accessibility of the node i for a given distance h is defined by the exponential of the Shannon entropy [19], i.e.,

$$\alpha_h(i) = \exp\left(-\sum_j P^{(h)}(i,j)\log P^{(h)}(i,j)\right), \tag{8}$$

where $1 \leqslant \alpha_h(i) \leqslant N$. The maximum value corresponds to the case in which all nodes are reached with the same probability $1/N$. Note that this metric was defined in a multilevel fashion, depending on the parameter h that defines the scale of the dynamics [19,20]. In addition, though here we will be constrained to random walks, virtually any other type of dynamics yielding transition probabilities between adjacent nodes can be considered in the accessibility, which makes this measurement adaptable to the dynamics of each problem being studied.

In order to generalize the accessibility, here we introduce a new version of this metric, which is based on the matrix exponential operation [22]. This matrix enables the calculus of the probability of transition considering walks of all lengths between any pair of vertices. In this way, if P is the transition matrix, the exponential of P is defined as

$$\mathbf{W} = \sum_{k=0}^{\infty}\frac{1}{k!}P^k = e^P. \tag{9}$$

The matrix $\mathbf{W}$ is based on a modified random walk, which penalizes longer paths. To construct such stochastic process we consider an usual random walk $(X_n)_{n\geqslant 0}$, where X_n represents the node visited by the agent at time n. We take a collection of independent and identically distributed uniform random variables in the interval $(0,1)$, i.e., $\{U_1, U_2, \ldots\}$, which represents a kind of "fitness" associated to each step of the walk. Also, we assume independence between the collection of uniform random variables and the random walk. This modified random walk, which we call accessibility random walk (ARW) in the rest of the paper, considers walks through the network such that all associated fitnesses along a trajectory are in ascending order. We say that node j is visited by the ARW, at time n, if $X_n = j$ and $U_1 < U_2 < U_3 < \cdots < U_n$. We denote by $(\tilde{X}_n)_{n\geqslant 0}$ the new process and note that $\{\tilde{X}_n = j\}$ implies $\{X_n = j\}$, but the opposite is not necessarily true. A quantity of interest is the number of visits that a given node j receives when an agent travels through the network according to the ARW. This quantity can be written as $\sum_{n=1}^{\infty} I_{\{\tilde{X}_n = j\}}$, where I_A is the indicator function of the event A. We are interested in the mean of this value by assuming that the agent starts from node i, i.e., $\sum_{n=1}^{\infty} E(I_{\{\tilde{X}_n=j\}}|\tilde{X}_0 = i)$. In order to compute this value we observe that the term of the sum is the probability $P(\tilde{X}_n = j|\tilde{X}_0 = i)$ which, by our definition, is equal to $P(\{X_n = j\} \cap \{U_1 < U_2 < U_3 < \cdots < U_n\}|X_0 = i)$. This probability is exactly $(1/n!)P^{(n)}(i,j)$, where $P^{(n)}(i,j)$ is the probability of transition from i to j through walks of length n. Therefore, the matrix $\mathbf{W}$ considered in Eq. (9) is a matrix of mean values associated to the ARW. The element $\mathbf{W}(i,j)$ provides the mean number of visits that node j receives when the agent starts at node i and follows the ARW.

The probability of transition between any pair of vertices through ARW is given by

$$\mathbf{P} = \frac{\mathbf{W}}{e}. \tag{10}$$

Note that the matrix $\mathbf{W}$ weights all walks by the inverse of the factorial of their lengths. Therefore, this definition penalizes longer walks, i.e., the shortest walks receive more weight than the longest ones. We define the generalized expression for the accessibility as

$$\alpha(i) = \exp\left(-\sum_j \mathbf{P}(i,j)\log\mathbf{P}(i,j)\right), \tag{11}$$

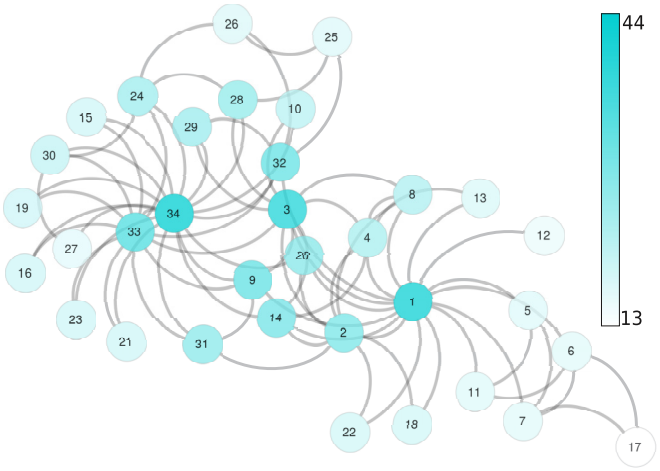

FIG. 1. (Color online) Illustration of the concept of the accessibility [values calculated from Eq. (11)] in the Zachary karate club network [21]. Nodes at the center of the network present the highest accessibility.

which we call generalized random walk accessibility. Figure 1 illustrates this measure.

We note that the exponential matrix is also considered in the definition of the communicability [23,24]. The difference is that the accessibility is based on the concept of diversity [25,26], whereas the communicability is associated to the communication between any pair of vertices [24]. Moreover, the former is related to the probability transition matrix, whereas the latter on the adjacency matrix. In this way, there is no trivial relation between these two measures in irregular graphs.

Let us provide in what follows some exact expression for the metric just introduced. Although the graphs considered below are not representatives of real-world networks, the analysis helps understanding what can be learned from the new metric. In addition, there are structures that already capture some important features of real networks, such as the star graph, which is an extreme example of an heterogeneous configuration, but that have provided insightful hints about the dynamics under study in other cases [27,28].

A. Accessibility in star graphs

For a star graph, the probability of transition between the central node i and any of the k leaves considering an ARW is given by [see Eqs. (9) and (10)]

$$\mathbf{P}(i,j) = \frac{1}{ek}\sum_{n=0}^{\infty}\frac{1}{(2n+1)!} = \frac{1}{ek}\sinh(1), \quad i \neq j, \tag{12}$$

and between the leaves and central node i,

$$\mathbf{P}(j,i) = \frac{\sinh(1)}{e}. \tag{13}$$

In addition,

$$\mathbf{P}(i,i) = \frac{\cosh(1)}{e}. \tag{14}$$

The probability of transition between leaves j and l is given by

$$\mathbf{P}(j,l) = \frac{1}{ek}[\cosh(1)-1], \tag{15}$$

and for $l = j$,

$$\mathbf{P}(j,j) = \frac{1}{e} + \frac{1}{ek}[\cosh(1)-1], \tag{16}$$

Therefore, the general form of the exponential matrix, considering the node number 1 as the hub of the star graph, is given as

$$\mathbf{P} = \frac{1}{e}\begin{bmatrix} \cosh(1) & \frac{1}{k}\sinh(1) & \cdots & \cdots & \frac{1}{k}\sinh(1) \\ \sinh(1) & 1+\frac{1}{k}[\cosh(1)-1] & \frac{1}{k}[\cosh(1)-1] & \cdots & \frac{1}{k}[\cosh(1)-1] \\ \vdots & \frac{1}{k}[\cosh(1)-1] & \ddots & & \vdots \\ \vdots & \vdots & & \ddots & \frac{1}{k}[\cosh(1)-1] \\ \sinh(1) & \frac{1}{k}[\cosh(1)-1] & \cdots & \frac{1}{k}[\cosh(1)-1] & 1+\frac{1}{k}[\cosh(1)-1] \end{bmatrix}. \tag{17}$$

In this way, since $k = N-1$, the accessibility of the hub i is

$$\alpha(i) = \exp\left[-x\log(x) - y\log\left(\frac{y}{N-1}\right)\right], \tag{18}$$

where $x = \frac{\cosh(1)}{e}$ and $y = \frac{\sinh(1)}{e}$. For any leaf j connected with i,

$$\alpha(j) = \exp[-x\log(x) + (N-2)y\log(y) + (1/e+y)\log(1/e+y)], \tag{19}$$

where $x = \frac{\sinh(1)}{e}$, $y = \frac{(\cosh(1)-1)}{e(N-1)}$.

We show in Fig. 2 the results obtained for the accessibility on top of different networks and configurations. As it can be seen, Eq. (18) can be considered to be a good predictor of the accessibility of the hubs in scale-free networks. However, as expected from the fact that the star graph does not capture any topological aspect of homogeneous networks, the star-graph approximation is not accurate for random Erdös-Rényi networks.

1. Eigendecomposition analysis

The exact values of accessibility in star graphs can also be calculated by the eigen-decomposition analysis of P. The exponential matrix, Eq. (9), can be obtained as

$$\mathbf{W} = e^{P} = \mathcal{V}\mathcal{D}\mathcal{V}^{-1}, \tag{20}$$

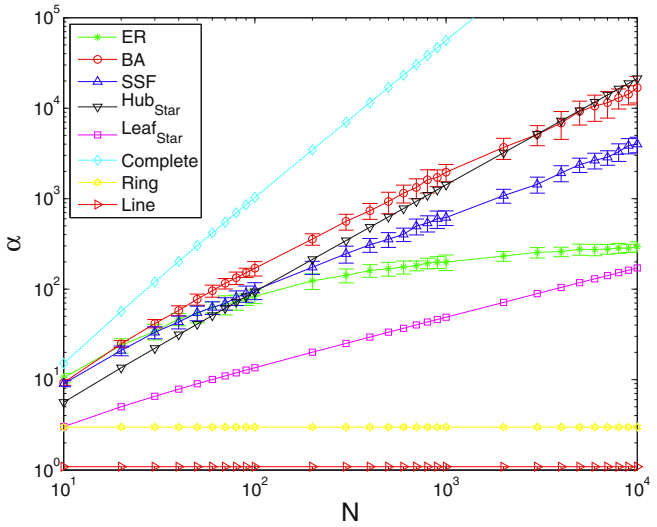

FIG. 2. (Color online) Accessibility calculated in star [from Eqs. (18) and (19)], complete, ring, and line graphs (extreme nodes) compared to the maximum value obtained in Erdös-Rényi (ER) random graphs, scale-free networks of Barabási-Albert (BA), and spatial scale-free networks (SSF). N is the network size. For complex networks, each point is an average over 50 networks with $\langle k\rangle \approx 4$.

where $\mathcal{V}$ is a matrix whose columns are the eigenvectors of the matrix $\mathbf{W}$ and $\mathcal{D}$ is a matrix whose diagonal presents the exponential of each eigenvalue of P,

$$(P - \lambda \mathbf{I})\, v = 0, \tag{21}$$

where P is the transition matrix, λ is its eigenvalue, and v is the associated eigenvector.

In this way, for the star graph, the transition matrix is sparse and its characteristic polynomial, $\det(P - \lambda I) = 0$, is calculated by the Laplace rule as

$$\begin{aligned}\det(P - \lambda I) &= (-\lambda)^N - (-\lambda)^{(N-2)} \\ &= (-\lambda)^{(N-2)}\left[(-\lambda)^2 - 1\right] = 0,\end{aligned} \tag{22}$$

whose solutions are $\lambda_1 = -1$, $\lambda_2 = 1$ and $\lambda_i = 0$, $\forall i = 2,3,\ldots,N$. Therefore, using the definition of an eigenvalue and eigenvector problem, it is possible to obtain the following equations for the eigenvectors. For $\lambda_1 = -1$,

$$\begin{aligned} v_{11} &= -\frac{1}{N-1}\sum_{j=2}^{N} v_{1j} \\ v_{1j} &= -v_{11}, \quad j = 2,3,\ldots,N, \end{aligned} \tag{23}$$

where v_{pj} is the j-th element of the eigenvector v_p associated with the eigenvalue λ_p. For $\lambda = 1$,

$$\begin{aligned} v_{21} &= \frac{1}{N-1}\sum_{j=2}^{N} v_{2j} \\ v_{2j} &= v_{21}, \quad j = 2,3,\ldots,N; \end{aligned} \tag{24}$$

finally, for $\lambda_p = 0$ where $p = 3,\ldots,N$, which has multiplicity $(N-2)$,

$$\begin{aligned} 0 &= \frac{1}{N-1}\sum_{j=2}^{N} v_{pj} \\ v_{p1} &= 0, \end{aligned} \tag{25}$$

which yields the matrix

$$\mathcal{V} = \begin{bmatrix} -1 & 1 & 0 & \cdots & \cdots & 0 \\ 1 & 1 & -1 & \cdots & \cdots & -1 \\ \vdots & \vdots & 1 & 0 & \cdots & 0 \\ \vdots & \vdots & 0 & \ddots & & \vdots \\ \vdots & \vdots & \vdots & & \ddots & 0 \\ 1 & 1 & 0 & \cdots & 0 & 1 \end{bmatrix}, \tag{26}$$

whose inverse is

$$\mathcal{V}^{-1} = \begin{bmatrix} \frac{-1}{2} & \frac{1}{2(N-1)} & \frac{1}{2(N-1)} & \cdots & \frac{1}{2(N-1)} \\ \frac{1}{2} & \frac{1}{2(N-1)} & \frac{1}{2(N-1)} & \cdots & \frac{1}{2(N-1)} \\ 0 & \frac{-1}{N-1} & \frac{N-2}{N-1} & & \frac{-1}{N-1} \\ \vdots & \vdots & & \ddots & \vdots \\ 0 & \frac{-1}{N-1} & \cdots & & \frac{N-2}{N-1} \end{bmatrix}. \tag{27}$$

Note that we used nonunit vectors to construct the matrices $\mathcal{V}$. This is not necessary since $\mathcal{D}$ is also multiplied by $\mathcal{V}^{-1}$ and the nonunit norms are compensated. Substituting in matrices (26) and (27) in Eq. (20), after some algebra, we recover Eq. (17). The accessibilty of hubs and leaves are calculated by Eqs. (18) and (19), respectively.

B. Accessibility in ring graphs

The generalized random walk accessibility can also be calculated exactly in rings that are a special case of K-regular graphs, where $K = 2$. The probability transition matrix has the form

$$P = \begin{bmatrix} 0 & \frac{1}{2} & 0 & \cdots & 0 & \frac{1}{2} \\ \frac{1}{2} & \ddots & \ddots & & & 0 \\ 0 & \ddots & \ddots & \ddots & & \vdots \\ \vdots & & \ddots & \ddots & \ddots & \vdots \\ 0 & & & \ddots & \ddots & \frac{1}{2} \\ \frac{1}{2} & 0 & \cdots & 0 & \frac{1}{2} & 0 \end{bmatrix}. \tag{28}$$

Such matrix has a well-known spectra and is widely used in finite difference methods [29]. As exposed in Ref. [29], the eigenvalues of P are

$$\lambda_p = \frac{1}{2}\left[\exp\left(\frac{2\pi i p}{N}\right) + \exp\left(\frac{-2\pi i p}{N}\right)\right] = \cos\left(\frac{2\pi p}{N}\right), \tag{29}$$

where $i = \sqrt{-1}$ and the associated elements of the eigenvector can be expressed as

$$u_{pj} = \frac{\exp\left(\frac{2\pi ipj}{N}\right)}{\sqrt{N}}, \tag{30}$$

where $\sqrt{N}$ is just a normalization factor. This set of eigenvectors diagonalizes the matrix P as $P = U\Lambda U^H$, where Λ is the diagonal matrix with the eigenvalues of P [Eq. (29)], U is the matrix whose columns are the eigenvector of P, and U^H is the conjugate transpose of U. We can write the closed expression for $\mathbf{P}$ as

$$\mathbf{P}(j,k) = \frac{1}{e}\sum_{p} \exp(\lambda_p) u_{pj} u^*_{pk}, \tag{31}$$

where u^*_{pj} is the conjugate transpose of u_{pj}. Note that we used the complex domain to solve the problem; however, the solution is on the real domain. Using Eqs. (29) and (30), we obtain

$$\mathbf{P}(j,k) = \frac{1}{eN}\sum_{p=1}^{N} \exp\left(\cos\left(\frac{2\pi p}{N}\right)\right) \exp\left[\frac{2\pi ip(j-k)}{N}\right], \tag{32}$$

which is a closed form for the evaluation of $\mathbf{P}$ in ring graphs. Furthermore we can use some graph spectra properties to separate the first eigenvalue from the summation

$$\mathbf{P}(j,k) = \frac{1}{e}\left(\frac{k_j}{2M}\right)\exp(1) + \frac{1}{N}\sum_{p=2}^{N} \exp\left\{\cos\left(\frac{2\pi p}{N}\right) + \left[\frac{2\pi ip(j-k)}{N}\right]\right\}. \tag{33}$$

Figure 2 shows the comparison between network models and the analytical solutions for the regular structures. Note that the solution for the ring does not depend on the network size. The results for the line graph, which again do not depend on the network size, are also presented in this figure. We also remark that the extremes of the line present the lowest values of accessibility, whereas the nodes in the center have the highest values.

C. Accessibility in complete graphs

The generalized random walk accessibility can also be calculated exactly for a complete graph, in which every pair of nodes is connected without self-connections. In this way, the probability of transition between any pair of nodes is $P(i,j) = \frac{1}{N-1}$ and the exponential matrix [see Eq. (9)] is given by

$$\mathbf{P}(i,j) = \frac{1}{eN}\sum_{n=0}^{\infty}\frac{(N-1)^n + (-1)^n(N-1)}{(N-1)^n n!} = \frac{\exp(1) + (N-1)\exp\left(\frac{-1}{N-1}\right)}{eN}, \quad i \neq j. \tag{34}$$

The main diagonal of $\mathbf{P}$, which considers the paths starting and ending at the same node, is expressed as

$$\mathbf{P}(i,i) = \frac{1}{eN}\sum_{n=0}^{\infty}\frac{(N-1)^n + (-1)^{n+1}}{(N-1)^n n!} = \frac{\exp(1) - \exp\left(\frac{-1}{N-1}\right)}{eN}. \tag{35}$$

Therefore, the general form of the exponential matrix is given as

$$\mathbf{P} = \frac{1}{e}\begin{bmatrix} \frac{\exp(1)+(N-1)\exp\left(\frac{-1}{N-1}\right)}{N} & \frac{\exp(1)-\exp\left(\frac{-1}{N-1}\right)}{N} & \cdots & \frac{\exp(1)-\exp\left(\frac{-1}{N-1}\right)}{N} \\ \frac{\exp(1)-\exp\left(\frac{-1}{N-1}\right)}{N} & \ddots & & \vdots \\ \vdots & & \ddots & \vdots \\ \frac{\exp(1)-\exp\left(\frac{-1}{N-1}\right)}{N} & \cdots & \cdots & \frac{\exp(1)+(N-1)\exp\left(\frac{-1}{N-1}\right)}{N} \end{bmatrix}. \tag{36}$$

The accessibility of each node is

$$\alpha(i) = \exp\{-\mathbf{P}(i,i)\log(\mathbf{P}(i,i)) + -(N-1)\mathbf{P}(i,j)\log(\mathbf{P}(i,j))\} = e(a^{-(N-1)a/e}b^{-b/e}), \tag{37}$$

where

$$a = \frac{1}{eN}\left[\exp(1) - \exp\left(\frac{-1}{N-1}\right)\right] \tag{38}$$

and

$$b = \frac{1}{eN}\left[\exp(1) + (N-1)\exp\left(\frac{-1}{N-1}\right)\right]. \tag{39}$$

In the complete graph all nodes present the same value of accessibility and, since a random walker needs just one step to reach any other node, this value is the upper bound of the maximum value of accessibility for a network with N nodes. Figure 2 shows the variation of the accessibility in complete graphs as a function of the network size.

1. *Eigendecomposition analysis*

The exact values of accessibility in complete graphs can also be obtained by the eigen-decomposition analysis, the graph spectra, and its eigenvectors, as performed for the star

graph. In this way, we get the following system [from Eq. (21)]:

$$\begin{bmatrix} -\lambda & \frac{1}{N-1} & \cdots & \frac{1}{N-1} \\ \frac{1}{N-1} & \ddots & & \vdots \\ \vdots & & \ddots & \vdots \\ \frac{1}{N-1} & \cdots & \cdots & -\lambda \end{bmatrix} v = 0, \tag{40}$$

which yields

$$\sum_{i,i\neq j}^{N} v_{pi}\left(\frac{1}{N-1}\right) - \lambda_p v_{pj} = 0, \quad \forall i,j;\ \ i \neq j, \tag{41}$$

where v_{pj} is the j-th element of the eigenvector v_p associated with the eigenvalue λ_p.

The eigenvalues of P for a complete graph is the spectrum of the adjacency matrix multiplied by $\frac{1}{N-1}$, i.e., $\lambda_1 = 1, \lambda_2 = \lambda_3 = \ldots = \lambda_N = \frac{1}{N-1}$ [30]. Therefore, for $\lambda_1 = 1$ we have

$$(N-1)\, v_{1j} = \sum_{i,i\neq j}^{N} v_{1i}, \quad \forall i,j;\ \ i \neq j. \tag{42}$$

The solution is $v_{1i} = v_{1j}$. On the other hand, for $\lambda_p = \frac{-1}{N-1}$, where $p = 2,3,\ldots,N$,

$$\sum_{i,i\neq j}^{N} v_{pi}\left(\frac{1}{N-1}\right) + \frac{1}{N-1} v_{pj} = 0, \tag{43}$$

i.e.,

$$\left(\frac{1}{N-1}\right)\sum_{i}^{N} v_{pi} = 0, \quad \forall i,j;\ \ i \neq j. \tag{44}$$

The respective solution is $\sum_i^N v_{pi} = 0$. Note that both solutions are not unique, whereas Eq. (20) has a unique solution. Without loss generality, we assume

$$\mathcal{V} = \begin{bmatrix} 1 & -1 & -1 & \cdots & -1 \\ 1 & 1 & 0 & \cdots & 0 \\ \vdots & 0 & \ddots & & \vdots \\ \vdots & \vdots & & \ddots & \vdots \\ 1 & 0 & \cdots & & 1 \end{bmatrix}, \tag{45}$$

whose inverse is

$$\mathcal{V}^{-1} = \begin{bmatrix} \frac{1}{N} & \frac{1}{N} & \frac{1}{N} & \cdots & \frac{1}{N} \\ \frac{-1}{N} & \frac{(N-1)}{N} & \frac{-1}{N} & \cdots & \frac{-1}{N} \\ \vdots & \frac{-1}{N} & \ddots & & \vdots \\ \vdots & \vdots & & \ddots & \vdots \\ \frac{-1}{N} & \frac{-1}{N} & \cdots & & \frac{(N-1)}{N} \end{bmatrix}. \tag{46}$$

Substituting matrices $\mathcal{V}$ and $\mathcal{V}^{-1}$ in Eq. (20) and using the information about the eigenvalues, we obtain the matrix in Eq. (36) and the same expression for the accessibility [Eq. (37)].

As a practical comment about the matrix exponential, it is important to mention that it should be computed by the Padé approximation [31,32] and not by the truncated Taylor series or by Eqs. (20). The former method is more precise and has a lower computational cost. However, Eq. (20) is important for theoretical analysis, since it transforms the calculus of accessibility into a eigenvector and eigenvalue problem, which is well studied in the literature.

IV. EPIDEMIC AND RUMOR SPREADING

Many mathematical models have been developed to study epidemic spreading in complex networks [33,34]. A particularly important model is the susceptible-infectious-recovered (SIR) model, in which each node can be in one of three states: (i) susceptible, (ii) infected, or (iii) recovered. Susceptible nodes are healthy and can catch the disease, whereas infected individuals are the ones actually transmitting the disease. Finally, individuals in the recovered state are immune to the disease and, therefore, play no role on the dynamics. The transitions between the first two states, i.e., from healthy to infected subjects, occurs via contacts between individuals. At each time step, the infectious nodes spread the disease to their susceptible neighbors with probability β and an infected node becomes recovered with probability μ. This is a spontaneous process and does not depend on any contact. The epidemic spreading process terminates when there is no infected node in the network and the disease cannot propagate anymore.

Rumor dynamics are in some aspects similar to epidemic spreading [35,36]. Rumor diffusion is simulated considering that nodes are spreaders, ignorants, or stiflers. Spreaders are those individuals that know the rumor and want to spread it to ignorants, whereas stiflers are those that know the rumor but are not interested in the information anymore. The main difference between rumor and epidemic spreading is that a spreader turns into a stifler by a process that involves contacts, whereas infected nodes become recovered by a spontaneous process. The fraction of ignorants ($\psi(t)$), spreaders ($\phi(t)$), and stiflers ($s(t)$) at time t are defined such that $\psi(t) + \phi(t) + s(t) = 1$. The process starts with one spreader and $N-1$ ignorants, where N is the number of nodes in the network. At each time step, spreaders try out to spread the rumor to their ignorant neighbors at a rate λ. On the other hand, if a spreader contacts another spreader or a stifler, such a spreader becomes a stifler at rate δ. This process corresponds to the model proposed by Maki and Thompson (MT model) [36]. In the version proposed by Daley and Kendall (DK model), two interacting spreaders become stiflers at rate λ [36]. Moreover, Monte Carlo simulations of a rumor spreading dynamics can be performed in two different ways. In a contact process (CP), only one random neighbor of a spreader is contacted at each time step. In the truncated process (TP) the neighbors of a spreader are contacted in a random way until all of them are contacted or the spreader turns into a stifler. The rumor dynamics terminates when there is no spreader in the network and the rumor cannot propagate anymore.

Here we consider that the spreading dynamics begin in a single seed node, whereas the remaining nodes are in the susceptible (or ignorant) state. In the SIR model, the spreading potential of each vertex is quantified in terms of the total prevalence of the epidemic process. The spreading capacity of i is the fraction of recovered vertices at the end of the process given that the dynamics started in i, i.e.,

TABLE I. Structural properties of the complex networks.

	Network	N	$\langle k\rangle$	$\langle \mathrm{cc}_i\rangle$	$\langle B_i\rangle$	$\langle C_i\rangle$	$\langle r_i\rangle$	$\langle \pi\rangle$	$\langle \alpha\rangle$	$\langle x_i\rangle$	$\langle k_c\rangle$
Spatial	Japan	2130	3.792	0.24	3.731×10^4	0.03	4.290	4.695×10^{-4}	6.95	2.892×10^{-3}	2.523
	England	4460	3.415	0.14	8.163×10^4	0.03	3.557	2.242×10^{-4}	6.65	1.401×10^{-3}	2.062
	United States	6443	3.098	0.09	1.605×10^5	0.02	3.302	1.552×10^{-4}	6.178	9.328×10^{-4}	2.038
	Germany	3555	3.068	0.08	5.944×10^4	0.03	3.173	2.813×10^{-4}	6.243	2.668×10^{-3}	1.988
	SpatialSF	5000	3.998	0.04	1.226×10^4	0.17	9.291	2.000×10^{-4}	9.793	6.001×10^{-3}	2.000
	Waxman	4883	4.078	0.14	4.598×10^4	0.05	4.863	2.048×10^{-4}	8.071	1.433×10^{-3}	2.570
Non-spatial	advogato	5054	15.58	0.25	5.748×10^3	0.31	9.962×10^1	1.979×10^{-4}	28.92	6.819×10^{-3}	8.137
	e-mail	1133	9.622	0.22	1.475×10^3	0.28	1.790×10^1	8.826×10^{-4}	17.88	1.764×10^{-2}	5.349
	Political blogs	1222	27.36	0.32	1.061×10^3	0.37	1.001×10^2	8.183×10^{-4}	33.08	1.681×10^{-2}	14.82
	Google+	23613	3.319	0.17	3.580×10^4	0.25	7.270×10^2	4.235×10^{-5}	15.13	2.301×10^{-3}	1.669
	BA	10000	3.999	5.76×10^{-3}	2.005×10^4	0.20	1.706×10^1	1.000×10^{-4}	10.57	3.108×10^{-3}	2.000

$M(i) = r(t \to \infty)$. Similarly, the spreading capacity of a node i in rumor dynamics is quantified by the percentage of stiflers at the end of the process given that the spreading started at i, i.e., $M(i) = s(t \to \infty)$.

V. DATABASE

We performed numerical simulations of epidemic and rumor spreading processes on top of real-world and artificial networks. Table I presents some network properties of the road maps and networks generated by the spatial models.

A. Network models

Barabási and Albert proposed a model which considers growth and preferential attachment rules [37]. In this case, a network is generated starting with a set of m_0 connected vertices. After that, new vertices with m edges are included in the network. The probability of the new vertex i to connect with a vertex j in the network is proportional to the number of connections of j, i.e.,

$$p(i,j) = \frac{k_j}{\sum_u k_u}. \tag{47}$$

The most connected vertices have greater probability of receiving new vertices. In this way, networks generated by this model present a power-law degree distribution, $P(k) = k^{-\gamma}$, where $\gamma = 3$ in the thermodynamic limit ($N \to \infty$) [37], N being the number of nodes.

We also take into account two spatial models. The model proposed by Waxman [38] considers that nodes are uniformly distributed into a square of unitary area and each pair of nodes is connected according to a probability that depends on their distances, i.e.,

$$p(i,j) = \eta \exp(-\eta d_{ij}), \tag{48}$$

where η is a parameter that controls the average degree and d_{ij} is the Euclidean distance between nodes i and j. Such model generates networks with an exponential degree distribution, which means that the probability of a node having a degree that differs from $\langle k\rangle$ decays exponentially.

The model introduced by Barthélemy [39], on the other hand, produces scale-free networks embedded in space. Considering a regular d-dimensional lattice with length L, the algorithm has three main steps. Initially, n_0 initial active nodes are selected at random. Next, an inactive node i is randomly selected and connected to an active node j with probability

$$p(i,j) \propto \frac{k_j + 1}{\exp(d_{ij}/r_c)}, \tag{49}$$

where k_j is the number of connections of node j, r_c is a finite scale parameter, and d_{ij} is the Euclidean distance between nodes i and j. Finally, the node i becomes active and the second and third steps are repeated until all nodes are active. For each node, the second and third steps are repeated m times in order to set the average connectivity as $\langle k\rangle = 2m$ [39]. The parameter r_c controls the clustering coefficient [40] and assortativity [9] of the network. Here we considered $r_c = 0.05$, $L = 1$, and $d = 2$. These values are similar to those used in the original paper [39].

B. Road networks

The road networks have been extracted from the maps available as a portable format (pdf) at the United Nations website. [1] Initially, the maps have been preprocessed in order to eliminate irrelevant information and keep only the main roads. After that, the skeletonization procedure has extracted the so-called skeleton of the image [41]. The node identification has been performed by applying an 8-connected hit-or-miss convolution filter [42]. Finally, a label propagation procedure has been implemented from each node. When two pair of labels i and j find each other, a connection is established between them. Here, we have considered the networks extracted from maps of Germany, Japan, England, and United States.

C. Social networks

The social networks considered here are as follows: (i) the email contact network obtained from messages exchanged between users within the Universitat Rovira i Virgili [43]; (ii) the political blogs network, composed of hyperlinks between web blogs obtained over the period of 2 months preceding the U.S. presidential election of 2004 [44]; (iii) the advogato network, which is an online community dedicated to free software development launched in 1999 [45,46]; and (iv) the Google+ network, which is composed by users connected

[1] http://www.un.org

according to their circles of friendships [47,48]. Avogato, political blogs, and Google+ networks are directed networks. Moreover, advogato is also a weighted network. However, here we consider only the unweighted and undirected versions of these networks. In addition, our analysis uses only the nodes in the giant component.

VI. PARAMETER ANALYSIS

The efficiency of a particular node in the spreading process depends not only on its topological characteristics but also on the parameters of the epidemic and rumor models. Here we calculate the above correlations between spreading capacity and the degree, k, k-core index, k_c, and accessibility, α, covering all possible combinations of parameters ($\beta \times \mu$ for epidemic spreading and $\lambda \times \delta$ for rumor propagation). Figure 3 shows the results for the road networks of the U.S. and Germany. The accessibility is the most correlated with the spreading capacity in all cases, whereas the k-core yields the smallest correlation for all set of parameters. On the other hand, the degree is most correlated with the spreading capacity in the SIR model for small values of β. In this case, the propagation reaches only the immediate neighbors of the infected node and, thus, the nodes with the largest degrees are the most efficient as far as the spreading is concerned. In addition, note that the correlation decreases for β close to 1, because the epidemics will succeed in reaching most of the nodes, regardless of the initial seeded node. For the rumor spreading, the correlation between the accessibility and the final fraction of stiflers is the highest for $\delta > \lambda$. The same relationship is observed for the degree, but the correlations are smaller than those observed for the accessibility measure.

Figure 4 shows the results for the social networks of email and political blogs cases. The results indicate that the degree, the k-core, and the accessibility yield similar correlations, which point out that the central nodes show the highest values of such measures simultaneously. Thus, these networks tend not to have peripheral hubs. The highest correlations occur for small values of β and λ, indicating that the infections or rumors do not propagate past the first neighbors of the origin and thus the nodes with the largest degree are the most efficient in spreading. These nodes also present the highest values of accessibility and k-core. For β and λ close to 1, the correlation is close to zero, because most of the nodes will become recovered or stifler independently of the initial spreader.

Having completed the previous analysis, we consider in the next sections the following parameter values: (i) $\beta = 0.8, \mu = 1.0$ and (ii) $\beta = 0.3, \mu = 1.0$ for the epidemic spreading and (i) $\lambda = 0.8, \delta = 1.0$, (ii) $\lambda = 0.8, \delta = 0.3$, (iii) $\lambda = 0.3, \delta = 1.0$, and (iv) $\lambda = 0.3, \delta = 0.3$ for the rumor dynamics. Note that previous investigations used $\delta = 1$ [12] and $\mu = 1$ [14] for

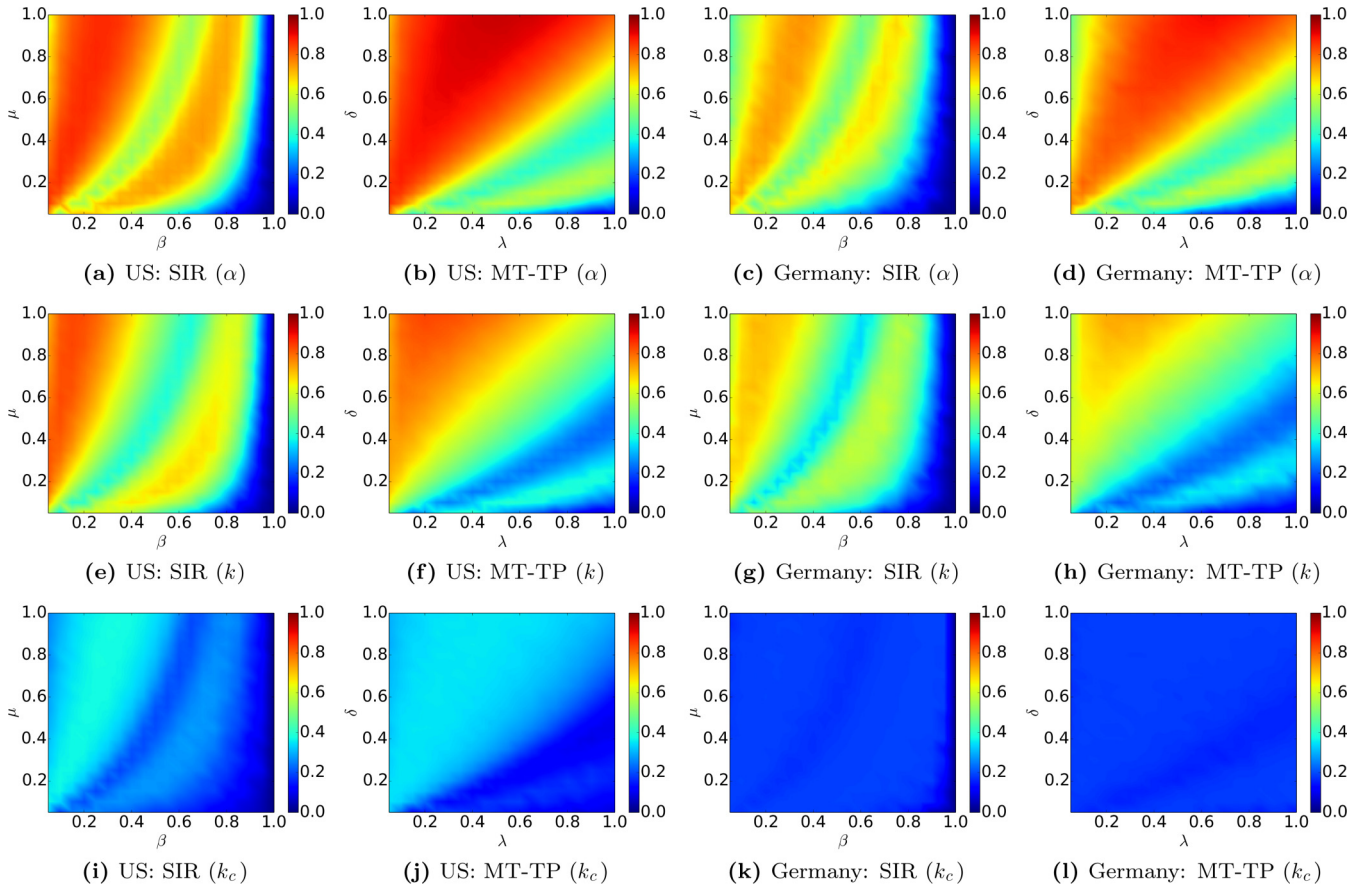

FIG. 3. (Color online) Correlation between spreading capacity and the degree, k, k-core index, k_c, and accessibility, α, covering all possible combinations of parameters ($\beta \times \mu$ for epidemic spreading (SIR model) and $\lambda \times \delta$ for rumor propagation (MT-TP model) for the road networks of US and Germany.

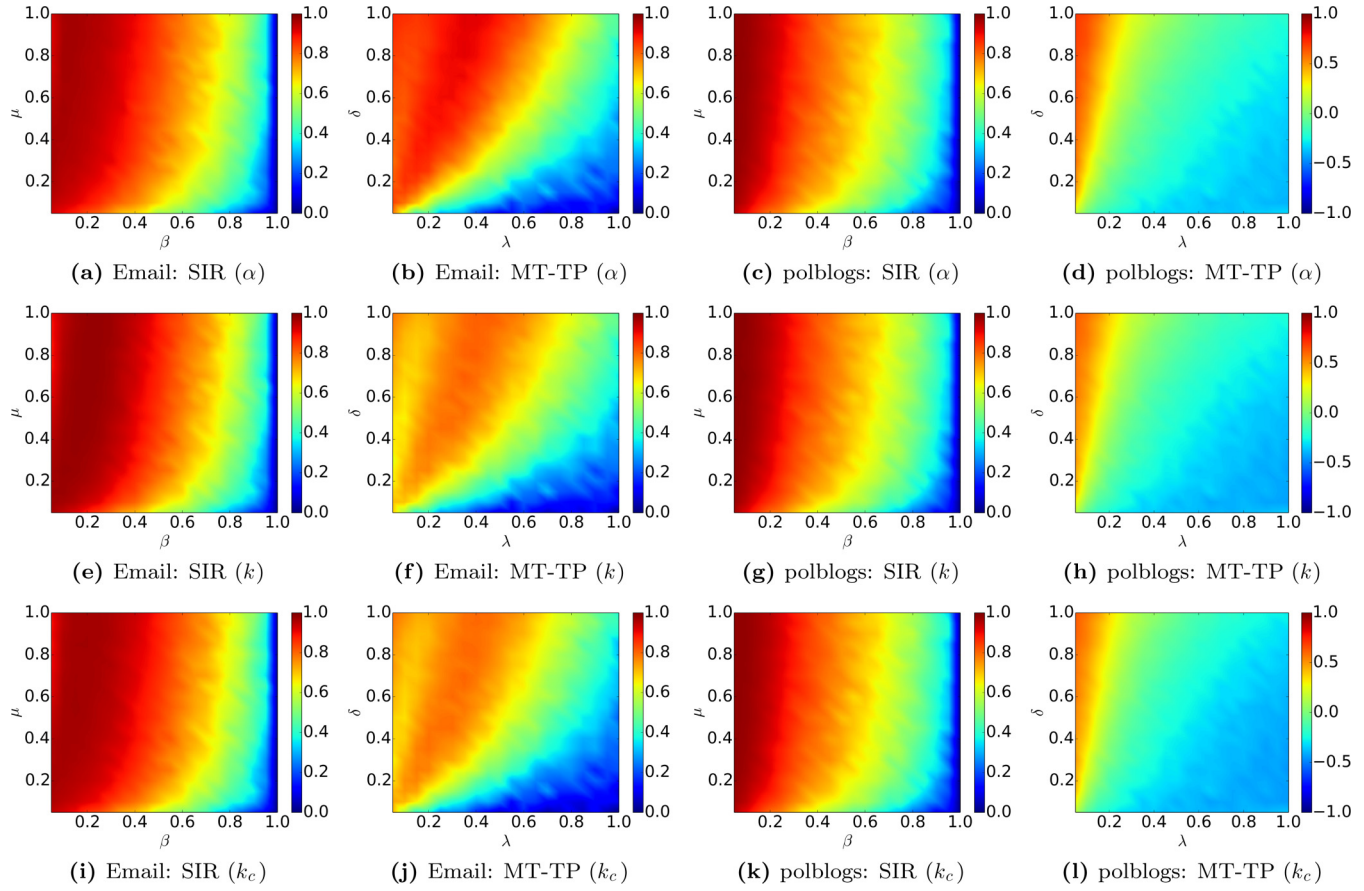

FIG. 4. (Color online) Correlation between spreading capacity and the degree, k, k-core index, k_c, and accessibility, α, covering all possible combinations of parameters ($\beta \times \mu$ for epidemic spreading (SIR model) and $\lambda \times \delta$ for rumor propagation (MT-TP model) for the email contact network and political blogs (polblogs).

epidemic and rumor spreading, respectively. Here, we consider also the cases in which the spreading rate is higher than the stifling rate and one situation in which both have the same values. These values represent the cases in which the dynamics are dependent on the network structure, i.e., correlations are higher than zero, as we can see in Figs. 3 and 4.

VII. SPATIAL NETWORKS

As outlined in Sec. II, we have studied different centrality metrics: the degree (k), clustering coefficient (cc), betweenness centrality (B), average neighborhood degree (r), PageRank (π), eigenvector centrality (x), k-core index (k_c), closeness centrality (C), and accessibility (α). We have considered only the unweighted and undirected versions of these measures. Table I presents the average values obtained for the road maps and networks generated by the Waxman and scale-free spatial models. Spatial networks are sparse and have large characteristic path lengths and nonzero clustering coefficients. In addition, scale-free spatial networks have the smallest average geodesic distance due to the presence of hubs.

We have conducted numerical simulations of the SIR (epidemic) and MT (rumor) models to inspect correlations between nodes' centrality (as given by the different metrics above) and the final dynamical outcome of the system, the latter being measured by the density of removed and stiflers after the dynamics has come to an end, respectively. Such correlations have been determined by the Spearman rank correlation coefficient, which is defined as the Pearson correlation coefficient between the ranked variables [49]. The reason of our choice is that the Spearman coefficient quantifies monotonic relationships, whereas the Pearson correlation measures linear relationships. As shown below, these correlations can be monotonic, but not necessarily linear.

Figures 5 and 6 show the scatter plots for the epidemic and rumor dynamics in the U.S. road network, respectively. The strongest correlation corresponds to the degree centrality, while for other metrics, correlations are weak and positive, though not zero. On the contrary, the clustering coefficient leads to a negative correlation because the more central a node is, the smaller its clustering coefficient is. On the other hand, Figs. 7 and 8 show that the correlations between the generalized random walk accessibility and the potential of rumor and epidemic spreading processes are almost linear and positive for all road networks analyzed.

Furthermore, Table II shows that for both spreading processes, the highest correlations between a centrality measure and the impact of the disease or rumor correspond to the case of the generalized accessibility centrality, which values often higher than 0.7. Interestingly, the k-core centrality yields small correlation values, contrary to what has been observed in Ref. [12], which considered networks not embedded in space.

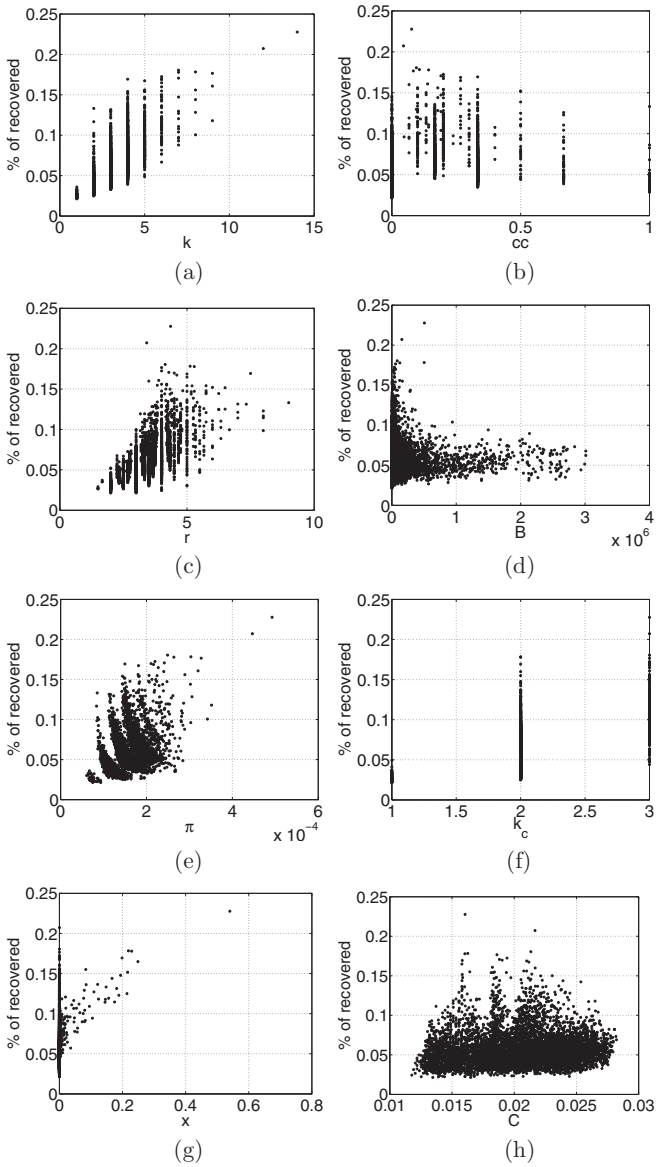

FIG. 5. The percentage of recovered individuals in the SIR epidemic spreading model ($\beta = 0.3, \mu = 1.0$) according to the local measures for the US road network: (a) degree; (b) clustering coefficient; (c) average degree of the nearest neighbors; (d) betweenness centrality; (e) PageRank; (f) k-core index; (g) eigenvector centrality; and (h) closeness centrality.

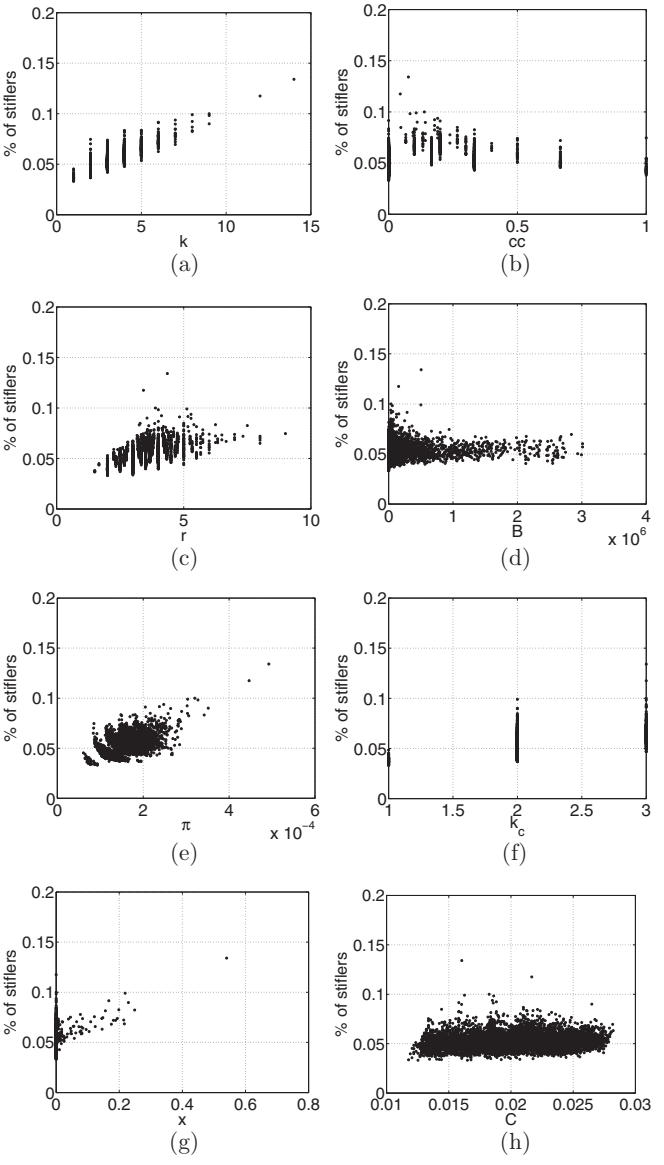

FIG. 6. The percentage of stiflers on the MT (TP) rumor model ($\lambda = 0.3, \delta = 1.0$) according to the local measures for the United States network: (a) degree; (b) clustering coefficient; (c) average degree of the nearest neighbors; (d) betweenness centrality; (e) PageRank; (f) k-core index; (g) eigenvector centrality; and (h) closeness centrality.

However, this result agrees with Ref. [14], in the case of rumor dynamics. The node degree is highly correlated with the final fraction of recovered nodes but less so if we look at the results corresponding to the final fraction of stiflers, mainly for the case of a MT model simulated using a contact process, as found in Ref. [14]. Moreover, PageRank, closeness, and betweenness centrality metrics do not show significant correlations with disease and rumor spreading capabilities, −except when the parameter δ in rumor models is small, in which case the closeness gives a high correlation. It is also worth noticing that the eigenvector centrality shows high correlation only for the spatial scale-free network model.

A. Road networks

Focusing on real networks, Fig. 9 shows results obtained for the generalized random walk accessibility of each node for the road networks of Japan, England, United States, and Germany. In Japan, the most influential spreaders are the cities of Nagoya, Osaka, and Hiroshima. Tokyo is highly connected, but does not have the same spreading capability of these cities, since it is a peripheral hub. London, Liverpool, and Manchester have the highest values of accessibility in England, while in the U.S., the cities with the highest accessibility are New York, Houston, Dallas, and Chicago, −interestingly enough, these cities are also air transportation hubs−. Finally, Berlin, München, and Düsseldorf have the highest accessibility in

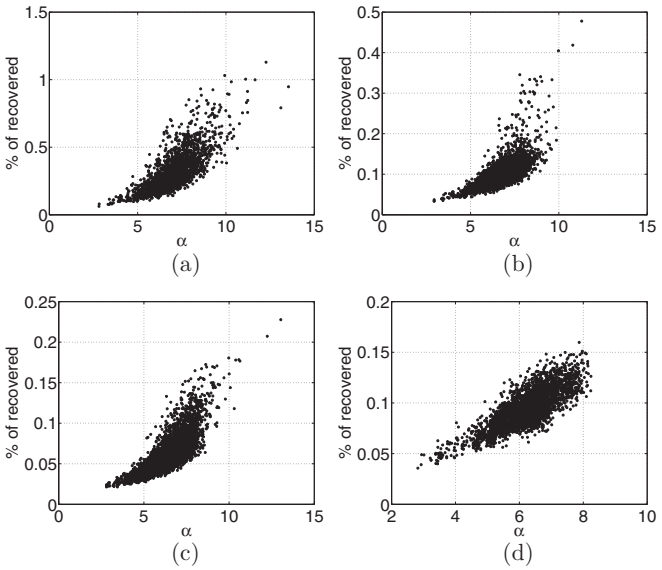

FIG. 7. The percentage of recovered individuals on the SIR epidemic spreading model ($\beta = 0.3, \mu = 1.0$) according to the accessibility measure for the road networks of (a) Japan, (b) England, (c) United States, and (d) Germany.

Germany. Note that nodes at the border of the countries present the smallest values of accessibility. Therefore, this measure can be considered for identification of border of networks, as previously pointed out for the original definition of accessibility in Ref. [20].

Figure 10 presents the probability distribution of the accessibility. For all cases, the distribution is asymmetric, presenting a long tail for higher values of accessibility and centered at the same value. It is interesting to note that Germany and England has the smallest variation in the accessibility, whereas Japan has the highest one. This fact can be related to the rough of Japan, which influence directly how highways are distributed.

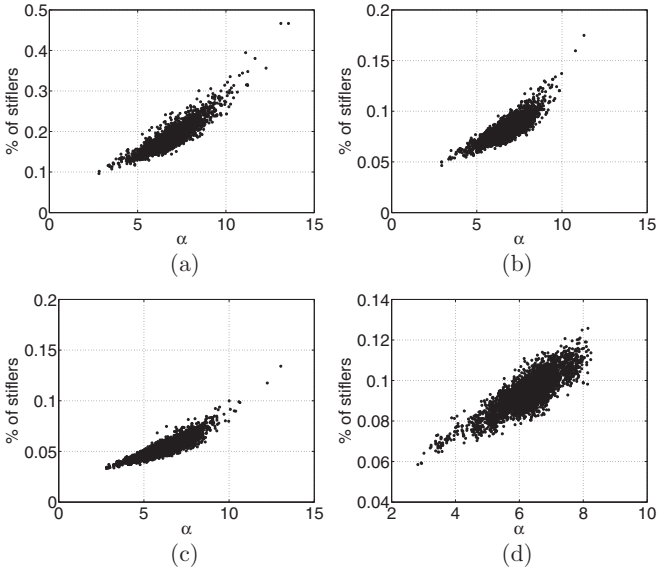

FIG. 8. The percentage of stiflers on the MT (TP) rumor model ($\lambda = 0.3$, $\delta = 1.0$) according to the accessibility measure for the road networks of (a) Japan, (b) England, (c) United States and (d) Germany.

VIII. NONSPATIAL NETWORKS

We have also studied what happens for nonspatial networks using the same set of measurements considered in Secs. VII and II. Table I presents the average values of these measures calculated in the social networks and in synthetic BA networks. Table III presents the Spearman correlation coefficient calculated between the centrality metrics and final fraction of stiflers or recovered nodes in the epidemic and rumor processes, respectively. The results agree with the analysis of epidemic spreading presented in Ref. [12] and with the study of rumor diffusion in Ref. [14]. In the case of the SIR model, the k-core and degree centralities are the most correlated with the final fraction of recovered nodes. Thus, the main hubs on the social networks are located in the center of the network, because they have the highest coreness, suggesting that such networks tend not to present peripheral hubs. Moreover, correlations are stronger when the parameter β is decreased. On the contrary, the random walk accessibility yields the highest Spearman correlation for BA networks and for political blogs (for $\beta = 0.3$), although the correlation values are close to those obtained for the degree and k-core. All the remainder metrics exhibit smaller correlation coefficients than the k-core, k, and α.

With respect to the rumor dynamics, the CP and TP cases present different results. In the first case, the eigenvector and accessibility centralities are strongly correlated with the final fraction of stiflers, whereas, for the second case, closeness centrality and average neighborhood degree show the highest correlations. Considering the TP case with a stifling rate $\lambda = 1$, if the spreading rate is high, the average neighborhood degree is more related to the dynamics. However, for lower spreading rates the distance from one node to the rest of the network is more critical. This property is evinced in Table III. Note that r presents higher correlations for higher spreading rates, whereas the closeness centrality is more correlated when spreading rates are smaller. Such an analysis suggests that shortest paths get more important for information propagation proportionally to the inverse of the spreading rate. Furthermore, the k-core and degree centralities have not been found to exhibit strong correlations with the final fraction of stiflers, supporting the results in Ref. [14]. Finally, we note that, at variance with previous cases, for the rumor dynamics on nonspatial networks, there is no single metric that has yielded the highest correlations for all the networks analyzed. In particular, the accessibility centrality does not seem to be in this case as distinct as before, likely because, as seen in Fig. 11, the distributions of accessibility in nonspatial networks are asymmetric, with different mean values and characterized by a long tail distribution.

IX. CONCLUSIONS

In this paper we have studied the relation between the centrality of a node and the outcome of epidemic and rumor processes initiated in that node by means of extensive numerical simulations on top of several complex networks. We have considered eight network centrality metrics and two

TABLE II. Correlation between centrality measures and the final fraction of recovered individuals (SIR model) or the final fraction of stiflers [MT model for the contact (CP) or truncated (TP) cases]. The measures are the degree (k), clustering coefficient (cc), betweenness centrality (B), average neighborhood degree (r), PageRank (π), eigenvector centrality (x), k-core index (k_c), closeness centrality (C), and accessibility (α). The highest correlations are in bold.

Process	Rates	Network	k	cc	B	r	π	x	k_c	C	α
SIR	$\beta = 0.8, \mu = 1.0$	Japan	0.40	0.11	0.24	0.26	0.27	0.27	0.35	**0.47**	**0.47**
		England	0.55	0.10	0.26	0.38	0.30	–0.04	0.21	0.27	**0.58**
		USA	0.60	0.25	0.19	0.53	0.28	0.49	0.26	0.41	**0.73**
		Germany	0.54	0.05	0.42	0.35	0.20	0.22	0.19	0.34	**0.63**
		SpatialSF	**0.81**	0.25	0.65	–0.04	0.75	0.35	–	0.32	0.60
		Waxman	**0.74**	0.34	0.47	0.29	0.62	0.05	0.70	0.19	**0.73**
	$\beta = 0.3, \mu = 1.0$	Japan	0.65	0.30	0.31	0.65	0.37	0.36	0.65	0.41	**0.79**
		England	0.68	0.13	0.27	0.61	0.31	–0.07	0.38	0.21	**0.76**
		USA	0.77	0.38	0.10	0.68	0.38	0.59	0.37	0.14	**0.86**
		Germany	0.69	0.08	0.46	0.42	0.31	0.22	0.19	0.25	**0.74**
		SpatialSF	0.70	0.39	0.70	0.46	0.49	0.72	–	0.66	**0.91**
		Waxman	0.68	0.30	0.42	0.58	0.45	0.04	0.72	0.30	**0.81**
MT-TP	$\lambda = 0.8, \delta = 1.0$	Japan	0.50	–0.08	0.43	0.48	0.29	0.33	0.45	0.42	**0.81**
		England	0.54	–0.20	0.43	0.49	0.22	–0.03	0.34	0.32	**0.85**
		USA	0.67	0.11	0.22	0.62	0.30	0.55	0.33	0.24	**0.90**
		Germany	0.57	–0.24	0.62	0.41	0.20	0.24	0.18	0.33	**0.88**
		SpatialSF	0.63	0.29	0.71	0.55	0.40	0.75	–	0.70	**0.94**
		Waxman	0.56	0.06	0.52	0.46	0.37	0.04	0.58	0.45	**0.76**
	$\lambda = 0.8, \delta = 0.3$	Japan	0.17	–0.02	0.22	0.23	0.04	0.26	0.21	**0.66**	0.35
		England	0.32	–0.07	0.31	0.38	0.05	0.05	0.26	**0.60**	0.53
		USA	0.26	0.00	0.25	0.29	0.07	0.08	0.12	**0.83**	0.43
		Germany	0.29	–0.12	0.46	0.28	0.01	0.45	0.17	**0.67**	0.52
		SpatialSF	0.40	0.16	0.43	0.28	0.27	0.41	–	0.37	**0.53**
		Waxman	0.61	0.13	0.51	0.38	0.47	0.06	0.62	0.31	**0.74**
	$\lambda = 0.3, \delta = 1.0$	Japan	0.77	0.22	0.43	0.61	0.54	0.25	0.59	0.28	**0.88**
		England	0.77	0.03	0.34	0.53	0.47	–0.07	0.30	0.16	**0.83**
		USA	0.84	0.32	0.19	0.63	0.50	0.56	0.35	0.13	**0.91**
		Germany	0.73	0.01	0.45	0.40	0.39	0.17	0.19	0.20	**0.79**
		SpatialSF	0.34	0.32	0.53	0.71	0.12	**0.89**	–	0.84	0.77
		Waxman	0.84	0.30	0.56	0.59	0.64	0.06	0.77	0.25	**0.94**
	$\lambda = 0.3, \delta = 0.3$	Japan	0.37	0.00	0.32	0.50	0.13	0.35	0.42	0.49	**0.68**
		England	0.42	–0.09	0.34	0.52	0.07	0.01	0.37	0.38	**0.71**
		USA	0.54	0.12	0.15	0.64	0.16	0.54	0.33	0.28	**0.80**
		Germany	0.42	–0.20	0.54	0.41	0.06	0.29	0.18	0.39	**0.73**
		SpatialSF	0.42	0.31	0.53	0.62	0.19	0.71	–	0.65	**0.84**
		Waxman	0.44	0.08	0.41	0.46	0.25	0.09	0.51	0.55	**0.64**
MT-CP	$\lambda = 0.8, \delta = 1.0$	Japan	0.42	0.05	0.30	0.57	0.16	0.32	0.48	0.42	**0.73**
		England	0.43	–0.10	0.32	0.56	0.08	–0.05	0.36	0.32	**0.73**
		USA	0.57	0.16	0.13	0.682	0.17	0.55	0.34	0.24	**0.82**
		Germany	0.45	–0.18	0.52	0.44	0.07	0.26	0.18	0.35	**0.75**
		SpatialSF	0.26	0.27	0.42	0.69	0.02	**0.75**	–	0.71	0.73
		Waxman	0.50	0.13	0.39	0.57	0.27	0.04	0.59	0.38	**0.72**
	$\lambda = 0.8, \delta = 0.3$	Japan	0.17	0.01	0.18	0.28	0.01	0.27	0.26	**0.67**	0.36
		England	0.24	0.00	0.24	0.37	–0.03	0.16	0.29	**0.70**	0.43
		USA	0.29	0.04	0.20	0.36	0.04	0.20	0.16	**0.74**	0.47
		Germany	0.20	–0.07	0.41	0.24	–0.05	0.51	0.16	**0.81**	0.40
		SpatialSF	0.28	0.22	0.36	0.46	0.10	0.48	–	0.44	**0.61**
		Waxman	0.54	0.16	0.44	0.55	0.34	0.10	0.64	0.44	**0.76**
	$\lambda = 0.3, \delta = 1.0$	Japan	0.60	0.18	0.36	0.66	0.34	0.28	0.56	0.31	**0.82**
		England	0.58	–0.02	0.31	0.60	0.25	–0.10	0.31	0.18	**0.77**
		USA	0.68	0.26	0.12	0.71	0.30	0.56	0.35	0.14	**0.85**
		Germany	0.55	–0.10	0.45	0.47	0.20	0.17	0.18	0.21	**0.74**
		SpatialSF	0.23	0.27	0.42	0.71	0.01	**0.81**	–	0.77	0.70
		Waxman	0.68	0.24	0.45	0.67	0.45	0.06	0.72	0.26	**0.87**
	$\lambda = 0.3, \delta = 0.3$	Japan	0.37	0.03	0.27	0.54	0.12	0.33	0.45	0.46	**0.68**
		England	0.40	–0.08	0.32	0.53	0.06	–0.01	0.36	0.36	**0.69**
		USA	0.54	0.14	0.13	0.65	0.14	0.53	0.33	0.27	**0.79**
		Germany	0.40	–0.20	0.52	0.43	0.03	0.27	0.18	0.39	**0.72**
		SpatialSF	0.27	0.27	0.43	0.67	0.03	0.71	–	0.66	**0.75**
		Waxman	0.44	0.10	0.38	0.51	0.23	0.05	0.53	0.46	**0.65**

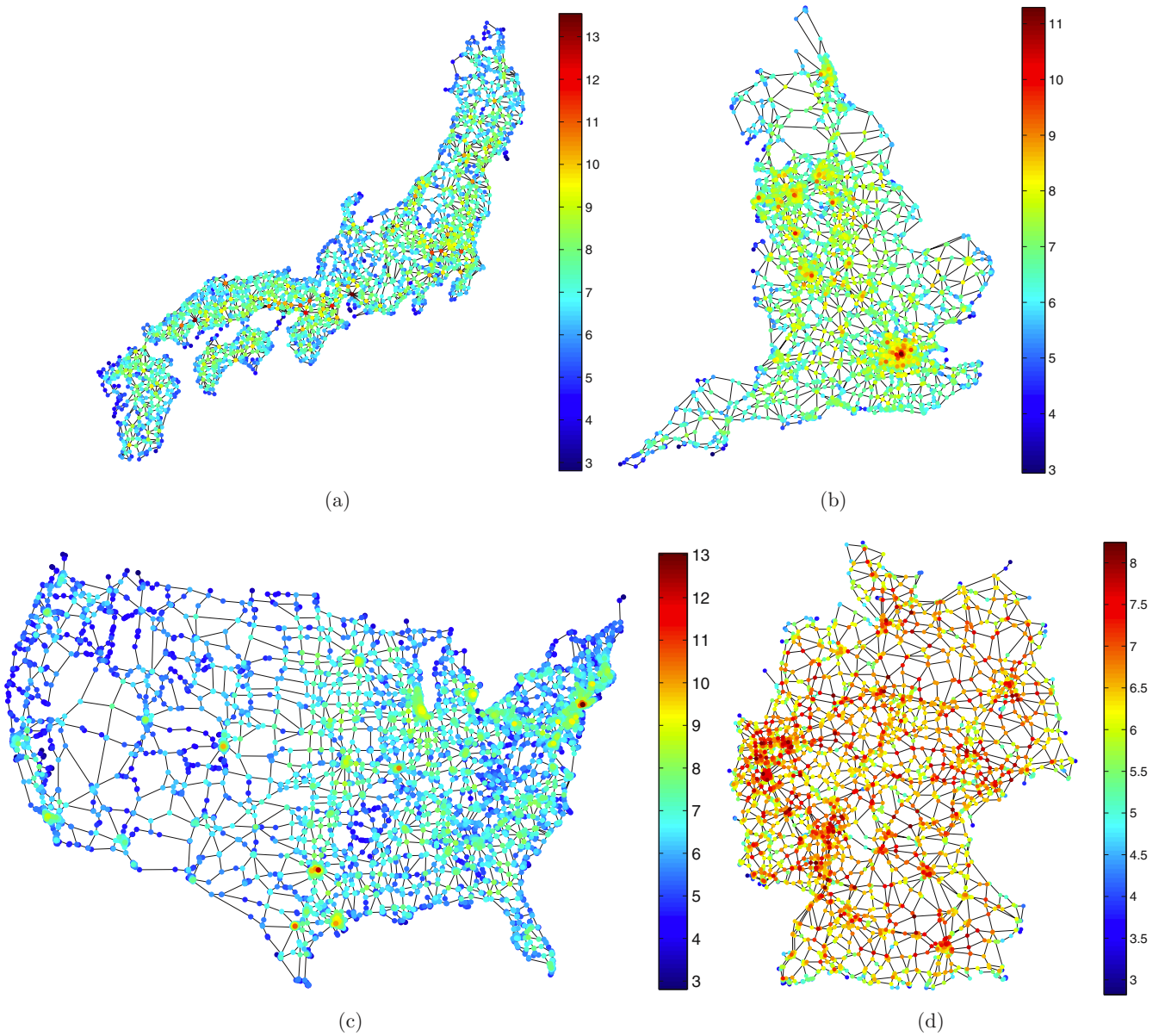

FIG. 9. (Color online) Network visualization of the real road networks of (a) Japan, (b) England, (c) United States, and (d) Germany. The colors represent the values of the accessibility.

different kinds of networks: spatial and nonspatial. Networks generated by the Barabási-Albert, Waxman, and scale-free spatial models have also been considered. We have proposed a generalization of the accessibility measure introduced in [19], which allows the quantification of the potential of each node in accessing in a balanced and homogeneous manner other nodes. Such generalization takes into account walks of all lengths weighted by the inverse of the factorial of their lengths.

Our results have shown that the generalized accessibility is the best metric to measure a node's spreading capacity in spatial networks. On the contrary, in nonspatial networks, the best correlations between a centrality metric and the dynamical outcome depends on the process. Thus, the degree and coreness (as given by the k-core) are the ones more suited when it comes to analyze epidemic spreading, confirming the results in Ref. [12]. However, these measures are not the best when a rumor model is considered. Indeed, for the latter case, the average neighborhood degree, the closeness centrality, and accessibility give higher correlations.

We verified that the generalized accessibility is more related to spreading processes in spatial networks than in nonspatial networks. Indeed, Table III shows that this metric is the structural property that exhibits the highest correlation in most of the cases when the underlying network is spatial. Figures 12 and 13 show that the relationship between the accessibility and centrality measures are almost linear in spatial networks, whereas in nonspatial networks, such a relationship is also almost linear but only for values below a given threshold. Beyond that value, the fraction of stiflers and recovered nodes

TABLE III. Correlation between centrality measures and the final fraction of stiflers [MT model for the contact (CP) or truncated (TP) cases] or recovered individuals (SIR model). The measures are the degree (k), clustering coefficient (cc), betweenness centrality (B), average neighborhood degree (r), PageRank (π), eigenvector centrality (x), k-core index (k_c), closeness centrality (C), and accessibility (α). The highest correlations are in bold.

Process	Rates	Network	k	cc	B	r	π	x	k_c	C	α
SIR	$\beta = 0.8.\mu = 1.0$	advogato	**0.76**	0.47	0.66	0.14	0.71	0.65	**0.76**	0.63	0.70
		email	**0.67**	0.41	0.57	0.09	0.64	0.58	**0.67**	0.57	0.63
		polblogs	**0.57**	0.29	0.51	0.04	0.55	0.55	**0.57**	0.55	**0.57**
		Google+	**0.81**	0.67	0.61	0.17	0.64	0.50	**0.81**	0.48	0.63
		BA	0.19	0.13	0.39	0.48	–0.02	0.45	–	0.49	**0.60**
	$\beta = 0.3.\mu = 1.0$	advogato	**0.97**	0.40	0.85	0.19	0.92	0.88	**0.97**	0.84	0.92
		email	**0.97**	0.34	0.85	0.25	0.94	0.88	**0.96**	0.89	0.94
		polblogs	**0.89**	0.25	0.78	–0.08	0.86	0.85	**0.89**	0.82	**0.88**
		Google+	**0.81**	0.67	0.61	0.23	0.60	0.56	**0.81**	0.54	0.68
		BA	0.18	0.18	0.48	0.73	–0.10	0.66	–	0.72	**0.77**
MT-TP	$\lambda = 0.8.\delta = 1.0$	advogato	0.23	0.17	0.26	**0.55**	0.17	0.38	0.22	0.43	0.35
		email	0.62	0.19	0.61	0.13	0.60	0.56	0.58	0.60	**0.64**
		polblogs	–0.16	–0.09	–0.06	**0.35**	–0.17	–0.16	–0.21	–0.07	–0.13
		Google+	0.04	0.03	0.00	**0.78**	–0.07	0.27	0.04	0.25	0.40
		BA	0.16	0.19	0.48	0.76	–0.12	0.70	–	0.75	**0.78**
	$\lambda = 0.8.\delta = 0.3$	advogato	0.05	0.15	0.10	0.51	0.02	0.20	0.05	**0.27**	0.16
		email	0.29	0.22	**0.30**	0.06	0.28	0.24	0.26	0.28	**0.30**
		polblogs	–0.37	–0.01	–0.26	**0.48**	–0.37	–0.34	–0.39	–0.22	–0.33
		Google+	0.00	0.03	–0.05	**0.69**	0.01	0.11	0.004	0.09	0.27
		BA	0.14	0.19	0.47	0.77	–0.11	0.79	–	**0.82**	0.72
	$\lambda = 0.3.\delta = 1.0$	advogato	0.54	0.11	0.47	0.64	0.45	0.74	0.55	**0.76**	0.73
		email	0.77	0.03	0.71	0.59	0.70	0.89	0.76	**0.91**	0.89
		polblogs	0.19	0.05	0.19	0.41	0.17	0.19	0.16	**0.31**	0.26
		Google+	0.20	0.17	0.14	**0.84**	–0.12	0.63	0.20	0.61	0.65
		BA	0.35	0.11	0.46	0.34	0.20	0.47	–	0.48	**0.51**
	$\lambda = 0.3.\delta = 0.3$	advogato	0.36	0.19	0.31	0.57	0.29	0.53	0.37	**0.57**	0.52
		email	0.70	0.19	0.62	0.35	0.65	0.71	0.70	0.74	**0.77**
		polblogs	–0.16	0.09	–0.12	**0.52**	–0.18	–0.13	–0.18	–0.02	–0.10
		Google+	0.14	0.16	0.05	**0.76**	–0.01	0.36	0.15	0.34	0.47
		BA	0.33	0.19	0.59	0.67	0.06	0.67	–	0.73	**0.85**
MT-CP	$\lambda = 0.8.\delta = 1.0$	advogato	0.47	0.14	0.35	0.52	0.36	0.63	0.50	0.62	**0.65**
		email	0.69	0.19	0.56	0.57	0.61	**0.81**	0.73	0.79	**0.81**
		polblogs	0.29	0.14	0.21	0.26	0.25	0.28	0.29	**0.34**	**0.34**
		Google+	0.40	0.32	0.31	0.55	–0.12	**0.84**	0.40	0.76	0.75
		BA	0.56	0.19	0.78	0.63	0.30	0.74	–	0.80	**0.94**
	$\lambda = 0.8.\delta = 0.3$	advogato	0.29	0.14	0.21	0.35	0.21	0.38	0.31	0.39	**0.41**
		email	0.45	0.22	0.36	0.32	0.40	0.48	0.47	0.50	**0.52**
		polblogs	0.01	0.14	–0.01	**0.26**	–0.03	0.02	0.00	0.07	0.05
		Google+	0.32	0.27	0.23	0.52	–0.10	**0.64**	0.33	0.60	0.64
		BA	0.24	0.21	0.58	0.80	–0.02	0.87	–	**0.91**	0.79
	$\lambda = 0.3.\delta = 1.0$	advogato	0.52	0.08	0.39	0.59	0.40	0.72	0.55	0.71	**0.73**
		email	0.64	0.05	0.55	0.68	0.55	**0.83**	0.67	0.82	0.80
		polblogs	0.51	0.14	0.39	0.25	0.46	0.52	0.51	0.56	**0.57**
		Google+	0.37	0.28	0.32	0.55	–0.15	**0.89**	0.38	0.84	0.75
		BA	**0.82**	0.10	0.67	–0.01	0.74	0.31	–	0.34	0.52
	$\lambda = 0.3.\delta = 0.3$	advogato	0.46	0.15	0.34	0.50	0.35	0.60	0.48	0.60	**0.63**
		email	0.68	0.23	0.55	0.50	0.60	0.76	0.71	0.76	**0.79**
		polblogs	0.19	0.14	0.13	**0.27**	0.15	0.18	0.18	0.24	0.23
		Google+	0.39	0.32	0.30	0.55	–0.11	**0.80**	0.40	0.74	0.74
		BA	0.67	0.19	0.79	0.49	0.43	0.66	–	0.72	**0.89**

reaches a plateau, which is the maximum value of the dynamic measure in the networks. Such a plateau reduces the Spearman correlation between the accessibility and the fraction of stiflers, since the relationship between these structural and dynamical measures is better defined for low values of accessibility. Therefore, due the higher distances in spatial networks, the value of accessibility does not saturate (i.e., there is no plateau), resulting in higher correlations.

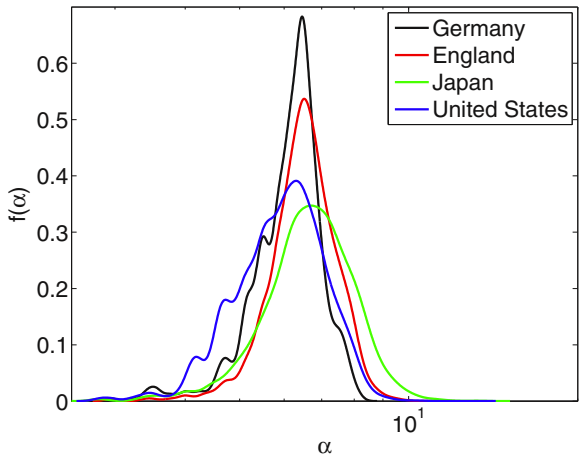

FIG. 10. (Color online) Probability distribution of the accessibility in the road networks of Japan, Germany, U.S., and England.

The previous conclusions can be understood by looking with more care to the meaning of the new metric here discussed. The definition of the accessibility in terms of random walks is strictly related to the spreading processes [50] and it is defined in terms of the diversity index of order one [25]. Thus, the higher the number of neighbors that a node can access with similar probability, the higher the expected number of infected nodes. In this way, the accessibility quantifies how many nodes can be effectively accessed during the spreading process. As reported in Ref. [51] this quantity is maximum whenever the exploration time is minimum. Thus, nodes presenting higher values of accessibility propagate viruses or rumors to the whole network faster than the nodes with smaller values, which results in a higher fraction of infected nodes before they become recovered. In summary, nodes with higher accessibility values should be the most influential spreaders.

The analysis presented here can be extended by considering other definitions of the accessibility in terms of other diversity indices [26]. The role of the generalized random walk

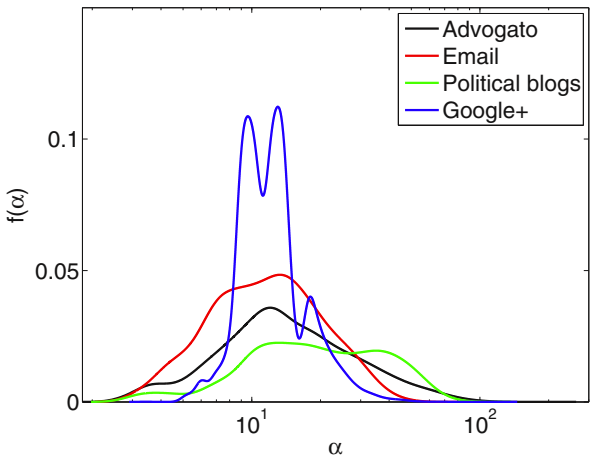

FIG. 11. (Color online) Probability distribution of the accessibility in the social networks of advogato, email, political blogs, and Google+.

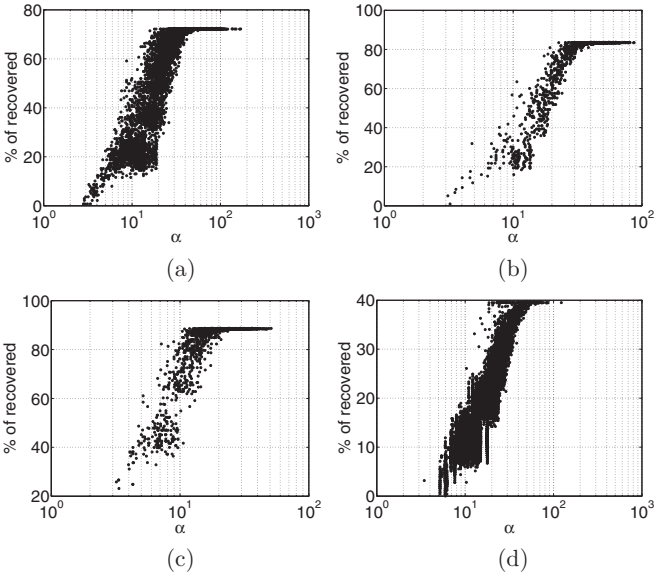

FIG. 12. Scatter plots of the accessibility measure and the final percentage of recovered individuals on the SIR epidemic spreading model ($\beta = 0.3, \mu = 1.0$) for the networks of (a) advogato, (b) political blogs, (c) email, and (d) Google+.

accessibility in other types of dynamical processes, such as social dynamic models [36] and synchronization, are also possible further studies. Ultimately, one important conclusion of our study, beyond the fact that the new metric appears to be the best way to detect influential spreaders in spatial networks, is that previous claims about whether a class of nodes are influential depends on both the metric used and, most importantly, on the kind of network under study.

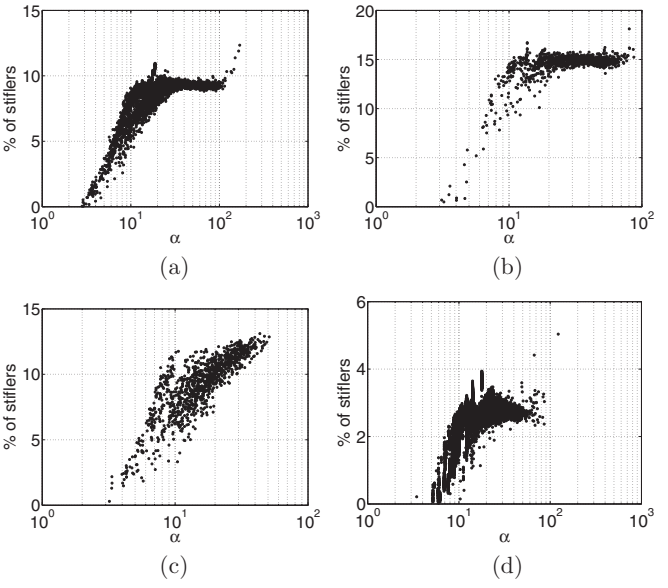

FIG. 13. Scatter plots of the accessibility measure and the final percentage of stiflers on the MT (TP) rumor model ($\lambda = 0.3, \delta = 1.0$) for the networks of (a) advogato, (b) political blogs, (c) email, and (d) Google+.

ACKNOWLEDGMENTS

F.A.R. acknowledges CNPq (Grant No. 305940/2010-4), Fapesp (Grant No. 2011/50761-2 and 2013/26416-9), and NAP eScience-PRP-USP for financial support. L.F.C. acknowledges CNPq and Fapesp for financial support. P.M.R. was supported by Fapesp (Grant No. 2013/03898-8) and CNPq (Grant No. 479313/2012-1). G.F.A. acknowledges Fapesp and A.L.B. acknowledges CAPES for sponsorship provided. Y.M. was partially supported by the EC FET-Proactive Project MULTIPLEX (Grant No. 317532).

[1] H. W. Hethcote, SIAM Rev. **42**, 599 (2000).
[2] L. da F. Costa, O. Oliveira Jr, G. Travieso, F. A. Rodrigues, P. R. V. Boas, L. Antiqueira, M. P. Viana, and L. E. C. Rocha, Adv. Phys. **60**, 329 (2011).
[3] A. Barrat, M. Barthlemy, and A. Vespignani, *Dynamical Processes on Complex Networks* (Cambridge University Press, New York, 2008).
[4] M. Newman, *Networks: An Introduction* (Oxford University Press, Oxford, 2010).
[5] L. Costa, F. Rodrigues, G. Travieso, and P. Boas, Adv. Phys. **56**, 167 (2007).
[6] S. Boccaletti, V. Latora, Y. Moreno, M. Chavez, and D. Hwang, Phys. Rep. **424**, 175 (2006).
[7] M. E. J. Newman, Phys. Rev. E **66**, 016128 (2002).
[8] R. Pastor-Satorras and A. Vespignani, Phys. Rev. Lett. **86**, 3200 (2001).
[9] M. E. J. Newman, Phys. Rev. Lett. **89**, 208701 (2002).
[10] M. Boguná, R. Pastor-Satorras, and A. Vespignani, Phys. Rev. Lett. **90**, 028701 (2003).
[11] Z. Liu and B. Hu, Europhys. Lett. **72**, 315 (2005).
[12] M. Kitsak, L. Gallos, S. Havlin, F. Liljeros, L. Muchnik, H. Stanley, and H. Makse, Nat. Phys. **6**, 888 (2010).
[13] R. A. P. da Silva, M. P. Viana, and L. da Fontoura Costa, J. Stat. Mech. Theor. Exp. (2012) P07005.
[14] J. Borge-Holthoefer and Y. Moreno, Phys. Rev. E **85**, 026116 (2012).
[15] S. Seidman, Soc. Networks **5**, 269 (1983).
[16] M. Barthélemy, Phys. Rep. **499**, 1 (2011).
[17] M. Girvan and M. Newman, Proc. Natl. Acad. Sci. USA **99**, 7821 (2002).
[18] S. Brin and L. Page, in *Computer Networks and ISDN Systems* (Elsevier Science, Amsterdam, 1998), pp. 107–117.
[19] B. A. N. Travençolo and L. da F. Costa, Phys. Lett. A **373**, 89 (2008).
[20] B. Travençolo, M. Viana, and L. d. F. Costa, New J. Phys. **11**, 063019 (2009).
[21] W. Zachary, J. Anthropol. Res. **33**, 452 (1977).
[22] R. Bhatia, *Matrix Analysis*, Vol. 169 (Springer-Verlag, Berlin, 1997).
[23] E. Estrada and N. Hatano, Phys. Rev. E **77**, 036111 (2008).
[24] E. Estrada, N. Hatano, and M. Benzi, Phys. Rep. **514**, 89 (2012).
[25] M. O. Hill, Ecology **54**, 427 (1973).
[26] L. Jost, Oikos **113**, 363 (2006).
[27] J. Gómez-Gardeñes, S. Gómez, A. Arenas, and Y. Moreno, Phys. Rev. Lett. **106**, 128701 (2011).
[28] Thomas Kauê Dal'Maso Peron and F. A. Rodrigues, Phys. Rev. E **86**, 016102 (2012).
[29] R. J. LeVeque, *Finite Difference Methods for Ordinary and Partial Differential Equations: Steady-State and Time-Dependent Problems* (SIAM, Philadelphia, PA, 2007).
[30] P. V. Mieghem, *Graph Spectra for Complex Networks* (Cambridge University Press, New York, 2011).
[31] G. H. Golub and C. F. V. Loan, *Matrix Computations* (The Johns Hopkins University Press, Baltimore, 1996), 3rd ed.
[32] N. J. Higham, SIAM J. Matrix Anal. Appl. **26**, 1179 (2005).
[33] M. J. Keeling and K. T. Eames, J. Roy. Soc. Interface **2**, 295 (2005).
[34] M. J. Keeling and P. Rohani, *Modeling Infectious Diseases in Humans and Animals* (Princeton University Press, Princeton, NJ, 2008).
[35] D. J. Daley, J. Gani, and J. M. Gani, *Epidemic Modeling: An Introduction* (Cambridge University Press, Cambridge, 2001), Vol. 15.
[36] C. Castellano, S. Fortunato, and V. Loreto, Rev. Mod. Phys. **81**, 591 (2009).
[37] R. Albert, Science **286**, 509 (1999).
[38] B. Waxman, IEEE J. Sel. Areas Commun. **6**, 1617 (1988).
[39] M. Barthélemy, Europhys. Lett. **63**, 915 (2003).
[40] D. J. Watts, *Small Worlds: The Dynamics of Networks between Order and Randomness* (Princeton University Press, Princeton, 1999).
[41] L. d. F. Costa and R. Cesar Jr, *Shape Analysis and Classification: Theory and Practice* (CRC Press, Boca Raton, FL, 2000).
[42] E. R. Dougherty, *An Introduction to Morphological Image Processing* (SPIE Optical Engineering Press, Bellingham, WA, 1992).
[43] R. Guimera, L. Danon, A. Díaz-Guilera, F. Giralt, and A. Arenas, Phys. Rev. E **68**, 065103 (2003).
[44] L. A. Adamic and N. Glance, in *Proceedings of the 3rd International Workshop on Link Discovery, LinkKDD'05* (ACM, New York, NY, 2005), pp. 36–43.
[45] P. Massa, M. Salvetti, and D. Tomasoni, in *Proceedings of the 8th IEEE International Conference on Dependable, Autonomic and Secure Computing (DASC'09)* (IEEE, Chengdu, China, 2009), pp. 658–663.
[46] Advogato network dataset—KONECT (2014), http://konect.uni-koblenz.de/networks/advogato.
[47] J. J. McAuley and J. Leskovec, in *Advances in Neural Information Processing Systems 25: 26th Annual Conference on Neural Information Processing Systems*, Proceedings of a meeting, Lake Tahoe, Nevada, December, 2012, edited by P. L. Bartlett, F. C. N. Pereira, C. J. C. Burges, L. Bottou, and K. Q. Weinberger (Curran Associates, Inc., Red Hook, NY, 2012), pp. 548–556.
[48] *Google+ network dataset—KONECT* (2014), http://konect.uni-koblenz.de/networks/ego-gplus.
[49] M. Hollander and D. A. Wolfe, *Nonparametric Statistical Methods* (John Wiley and Sons, New York, NY, 1973).
[50] P. C. Pinto, P. Thiran, and M. Vetterli, Phys. Rev. Lett. **109**, 068702 (2012).
[51] M. P. Viana, J. L. B. Batista, and L. d. F. Costa, Phys. Rev. E **85**, 036105 (2012).